DETECTING BRAIN SHIFT DURING DEEP BRAIN STIMULATION SURGERY USING INTRA-OPERATIVE DATA AND FUNCTIONAL ATLASES: A PRELIMINARY STUDY

Srivatsan Pallavaram[1], Pierre-François D'Haese[1], Michael S. Remple[2], Joseph S. Neimat[2], Chris Kao[2], Rui Li[1], Peter E. Konrad[2], Benoit M. Dawant[1]

[1] Dept. of Electrical Engineering & Computer Science, Vanderbilt University, Nashville, TN, USA
[2] Dept. of Neurosurgery, Vanderbilt University Medical Center, Nashville, TN, USA

ABSTRACT

Recently, many groups have reported on the occurrence of brain shift in stereotactic surgery and its impact on the procedure. A shift of deep brain structures by only a few millimeters can potentially increase the number of required microelectrode and/or macroelectrode tracks. This can cause complications and potentially affect implantation accuracy. Detecting intra-operative brain shift and, more significantly correcting for it intra-operatively can thus impact the procedure and its outcome. In this study, we have used intra-operative stimulation response data to assess brain shift. Using a shift free functional atlas containing therapeutic response to stimulation (efficacy) data from a population of patients we build statistical efficacy maps on new patients. We then compare the information provided by the maps with the actual intra-operative responses of those patients to detect brain shift. Our preliminary results show that by maximizing the correlation between statistical maps and intra-operative observations, it may be possible to detect intra-operative brain shift and potentially correct for it.

Index Terms— Deep brain stimulation, intra-operative brain shift, statistical maps, functional atlases

1. INTRODUCTION

Deep brain stimulation (DBS) is a surgical procedure involving the implantation of an electrode in the deep brain to stimulate specific nuclei using a pacemaker. DBS has provided remarkable therapeutic benefits to patients suffering from movement disorders such as the Parkinson's disease. Because of the small size of the nuclei and the potential shift of the deep brain structures due to air invasion, such neurosurgical procedures are traditionally performed in two stages. A target location is first selected pre-operatively by a neurosurgeon and then refined intra-operatively using multiple exploratory electrodes to map the electrophysiology of the brain around the planned target. Although intra-operative electrophysiological techniques such as micro-electrode recording and stimulation can be used to compensate for it, brain shift can lengthen the procedure and cause complications.

For years, neurosurgeons and researchers have investigated the value of tracking brain shift during surgery for invasive procedures such as brain tumor resection [1, 2]. Recently, several groups have reported on the significance of brain shift in DBS surgeries. Miyagi *et al.* [3] reported contralateral and posterior shift at the anterior and posterior commissures. Khan *et al.* [4] analyzed brain shift between pre-operative and post-operative 3D MRI scans in 25 subjects. They reported brain shifts of up to 4 mm in deep brain structures. In a 2008 study, Halpern *et al.* [5] reported comparable results where shift impacted the number of microelectrode tracks needed to optimize targeting. Therefore, if brain shift can be detected intra-operatively in DBS surgery, it may reduce the length of the procedure and guide the surgeon in identifying the optimal target using fewer exploratory electrodes. In this study we describe a method to build functional atlases by taking brain shift into account and use them to detect intra-operative brain shift.

2. DATA

2.1 Image data

With IRB approval each patient had pre-operative MRI and CT, and a post-operative CT acquired on the day of the surgery. Typical CT images were acquired at kVp = 120 V, exposure = 350 mAs and 512x512 pixels. In-plane resolution and slice thickness were respectively 0.5 mm and 0.75 mm. MRI (TR 12.2 ms, TE 2.4 ms, 256x256x170 voxels, with typical voxel resolution of 1x1x1 mm³) were acquired using the SENSE parallel imaging technique (T1W/3D/TFE) from Philips on a 3T scanner.

At our institution the surgery is performed with a patient customized miniature stereotactic frame, the StarFix microTargeting Platform® (501(K), Number K003776, Feb. 23, 2001, FHC, INC; Bowdoin, ME) instead of a standard stereotactic frame. During surgery, a micro-positioning drive (microTargeting® drive system, FHC Inc., Bowdoin, ME) is mounted on the platform to guide recording and stimulating electrodes to the target.

2.2 Stimulation response data

In this study, we used patients that underwent sub-thalamic nucleus (STN) targeting. Stimulation response data included the location of each stimulation point, the efficacy (therapeutic response) observed and the associated stimulation current, the side effect (if any) and the associated current. We have only used efficacy data in this study. Efficacy was recorded as percentage reduction in symptoms from baseline as assessed by a neurologist. Only those points with at least 70% efficacy were used. The

dataset comprised of 55 efficacious points from 12 patients for the left side and 48 efficacious points from 12 patients for the right side.

3. METHOD

3.1 Registration
A key component of the method is our ability to map information acquired from a population of patients onto one reference image volume, termed the atlas. This has been demonstrated in our earlier works [6-8]. We can also map the atlas onto a patient in the same way. Two types of registrations algorithms are needed to perform such mapping; rigid and non-rigid. The rigid registration algorithm is required to align pre-operative MRI and CT scans. Non-rigid registration is required to map patient data onto the atlas. In this study, non-rigid registration is always performed on MRI volumes using the adaptive bases algorithm we have proposed earlier [9]. Both the rigid and non-rigid registration algorithms are based on mutual information.

3.2 Creating brain shift free functional atlases and statistical maps
Each post-operative CT was carefully inspected for pneumocephalus and each patient was categorized into *low* and *large* brain shift. We used only *low* and *large* shift patients in this study to demonstrate the proof of principle of the proposed method on data that have clearly different brain shifts. Patients with average air pocket width at lead level less than or equal to 3 mm were in the *low category*, and those with average air width greater than 7 mm in the *large* category. The air pockets were measured from the inner table of the calvarium in the frontal cortex as shown in fig 1. In order to account for brain shift, only the data from patients in the *low* shift category were used to create the shift free functional atlases.
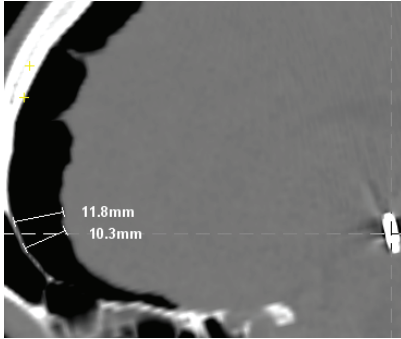
Fig 1 Frontal portion of a sagittal slice in a post-operative CT scan containing the lead and showing an air pocket. Width of the air pocket is measured from the inner table of the calvarium at the lead level. Two sample measurements (11.8 mm and 10.3 mm) are shown for a *large* shift case.

For every stimulation point; the depth of the electrode was read from the micro-positioning device and converted into X, Y, and Z coordinates in the pre-operative CT space. The patient pre-operative MRI and CT images were registered using a rigid body registration. Each MRI volume was then registered to the atlas through non-rigid registration. The transformations were concatenated and the X, Y, and Z coordinates of the intra-operative data were transformed into X_A, Y_A, and Z_A atlas coordinates. This way the atlas was populated using data from a number of patients. Using the inverse procedure, the atlas data coordinates were transformed into patient X^*, Y^*, and Z^* coordinates.

The statistical efficacy maps were built using the method described in detail in [6]. Briefly, we assume that responsive neurons are localized somewhere on a sphere centered on the stimulation point with the radius of the sphere proportional to stimulation voltage or current causing the response. If response was observed at stimulation current I, then we consider that the responsive neurons were activated between current $I–\varepsilon$ (radius r_2) and I (radius r_1) where ε is a positive real number. Thus, we assume that the responsive neurons lie on this annulus or a spherical shell in 3D. We associate a uniform probability density function with the neurons in this annulus. Summing over a number of such stimulation points and normalizing yields a map of responsive stimulation regions. Our current to radius relationship is based on the data published by Butson *et al.* [10] for mono-polar stimulation using a DBS electrode with standard stimulator settings in an isotropic medium.

Specifically, for a point $P_1(X^*, Y^*, Z^*)$ on a patient, a spherical shell-based stimulation map is created as follows. Let Ω_1 be the set of all voxels inside the spherical shell (equation (1)). The value of the map at a point with coordinates (x^*, y^*, z^*) in the image due to the observation at P_1 is $F_{P1}(x^*, y^*, z^*)$ defined in equation (2).

$$\Omega_1 = \{(x^*, y^*, z^*) \in R^3 \mid r_2^2 < (x^* - X^*)^2 + (y^* - Y^*)^2 + (z^* - Z^*)^2 \leq r_1^2 \quad (1)$$

$$F_{P_1}(x^*, y^*, z^*) = \left\{ \frac{1}{n(\Omega_1)} when (x^*, y^*, z^*) \in \Omega_1, 0\ otherwise \right\} \quad (2)$$

$n(\Omega_1)$ *is the number of elements in the set* Ω_1

When multiple points P_1, P_2… P_N are used in building a map, the overall efficacy map F at any point (a, b, c) is defined as in equation (3).

$$F(a,b,c) = \frac{1}{N} * \left(\sum_{i=1}^{N} F_{P_1}(a,b,c) \right) \quad (3)$$

3.3 Assessment of brain shift using statistical efficacy maps and patient-specific intra-operative efficacy data
In order to detect brain shift using functional maps, we first validate the assumption that the efficacy maps generated for *low* shift patients using the shift free functional atlas correlate well with the intra-operative recordings for those patients. We then use such maps to detect shift in *large* brain shift patients.

To investigate the correlation between the map and actual observations in *low* shift patients, the patients were chosen such that at least one of the stimulation tracks went through the map. Then, we used efficacy maps to assess intra-operative brain shift in *large* shift patients by comparing the maps with their intra-operative data.

4. RESULTS

In this study we have used four patients to test our hypothesis. Two patients (*Low1*, *Low2*) were in the *low* shift category and two (*Large1*, *Large2*) in the *large*. Efficacy maps are shown in 2D. The scale is shown in fig 2(b).
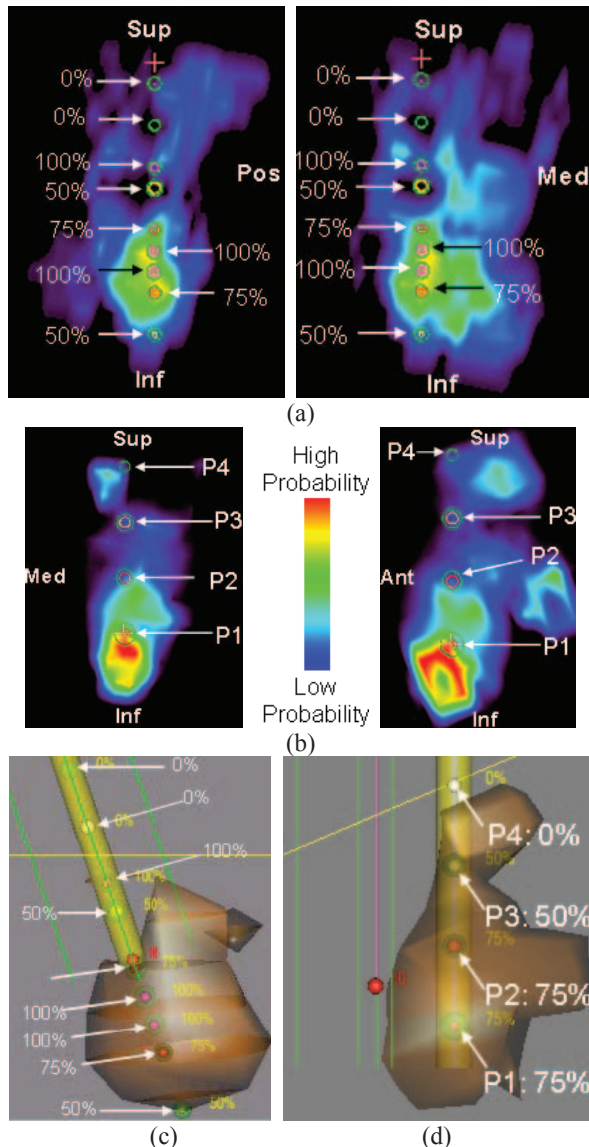
Fig 2 Sagittal and coronal slices of atlas-generated efficacy maps two low shift patients (a) *Low1*, (b) *Low2* with their intra-operative observations overlaid. The corresponding

3D rendering of the map isosurfaces are in (c) and (d). The common color scale is shown in (b).

In the 3D renderings, each data point is represented by a sphere with the radius of the sphere proportional to the current causing the response. Efficacious points are represented by solid spheres with the color or gray level (same scale as the maps) indicating the degree of efficacy while points producing no efficacy are shown as solid white spheres. If a side effect occurs it is represented by a semi-transparent sphere. The cylindrical tube in each 3D view represents the most efficacious trajectory while the other trajectories are shown as lines parallel to it.

Sagittal and coronal slices of the atlas-generated efficacy maps with overlaid intra-operative observations from two *low* shift patients *Low1* and *Low2* are shown in fig 2(a) and 2(b) respectively. The 3D renderings of the corresponding map isosurfaces are shown in fig 2(c) and 2(d). Fig 3(a) shows the 3D rendering of the atlas-generated statistical efficacy map for patient *Large1* along with the intra-operative observations for the patient. The axial slices of the map containing high efficacy observations P1 and P2 are shown in fig 3(b).
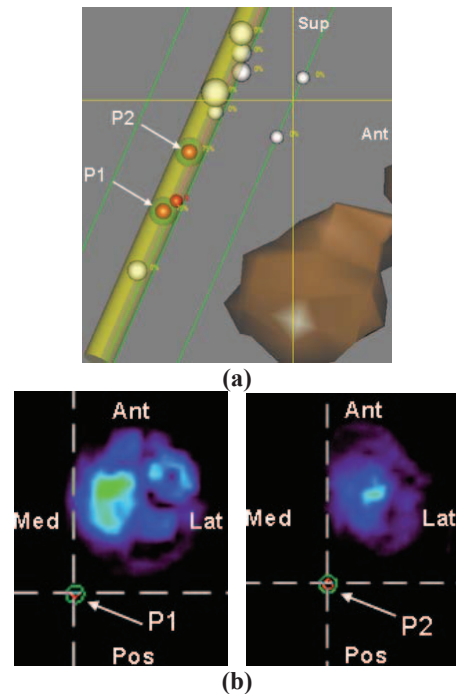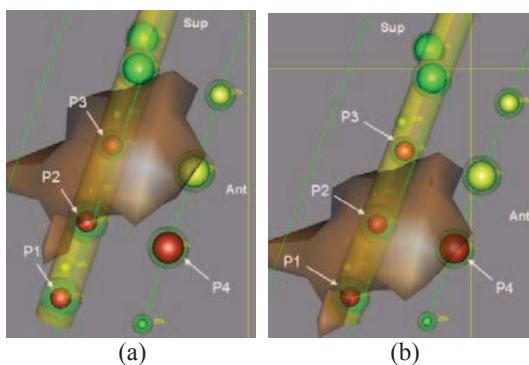
Fig 3 (a) 3D rendering of the efficacy map for a large shift patient *Large1* with the actual stimulation response points overlaid. P1 and P2 are high efficacy observations. (b) Axial slices of the map containing P1 and P2.

5. DISCUSSION

Fig 2 shows that the efficacy maps correlate well with the intra-operative recordings in *low* shift patients. It can be

seen in fig 2(a) that four of the five high efficacy observations (>=70%) for *Low1* lie in the high probability region of the map (hot zone) and all the low efficacy observations lie outside the high probability region. Similarly, for *Low2*, the low efficacy observations P3 (50%) and P4 (0%) lie outside the hot zone and the high efficacy observations P1 (75%) and P2 (75%) lie inside the hot zone as shown in fig 2(b).

Fig 3 illustrates a *large* shift patient's case. The high efficacy data points P1 and P2 in fig 3(a) are respectively 4.64 mm and 5.18 mm away from the hot zone in the map and are posterior and medial to it. This suggests that the anatomical region producing efficacy had shifted posterior and medial.

(a)   (b)

Fig 4 Intra-operative observations for a large shift patient *Large2* overlaid on top of the 3D rendering of the atlas-generated efficacy map (a) before shifting the, (b) after shifting the map 2mm inferior map to match data. P1, P2, P3, P4 are high efficacy observations.

A similar trend can be seen in fig 4(a) for the second *large* shift patient *Large2*. To illustrate brain shift in this case, the map was manually shifted 2 mm inferior as shown in fig 4(b). Comparing 4(a) and 4(b) corroborates our finding. The map in fig 4(b) is more consistent with the observed intra-operative data than the map in fig 4(a). Thus, this shift is a good estimate of the brain shift and the correction needed to be applied to the functional map to account for brain shift. The normalized map values at points P1, P2, P3 and P4 shown in fig 4(a) are 0.19, 0.38, 0.90 and 0.10. The values at the same points after shifting the map as in fig 4(b) are 0.38, 0.90, 0.50 and 0.43. This suggests that by maximizing the correlation between the statistical map and patient specific intra-operative observations brain shift could be estimated.

Although preliminary, the results we have obtained indicate that an electrophysiological atlas could be used during the procedure to estimate brain shift and to provide intra-operative guidance for DBS lead placement.

6. ACKNOWLEDGEMENT

7. REFERENCES

[1] D. W. Roberts, A. Hartov, F. E. Kennedy, M. I. Miga, and K. D. Paulsen, "Intraoperative brain shift and deformation: a quantitative analysis of cortical displacement in 28 cases," *Neurosurgery,* vol. 32 (4), p. 749:760, 1998.

[2] M. I. Miga, K. D. Paulsen, J. M. Lemery, S. Eisner, A. Hartov, F. E. Kennedy, and D. W. Roberts, "Model-updated image guidance: Initial clinical experience with gravity-induced brain deformation," *IEEE Transactions on Medical Imaging,* vol. 18 (10), p. 866:874, 1999.

[3] Y. Miyagi, F. Shima, and T. Sasaki, "Brain shift: an error factor during implantation of deep brain stimulation electrodes," *Neurosurgery,* vol. 107, pp. 989–997, 2007.

[4] M. F. Khan, K. Mewes, R. E. Gross, and O. Škrinjar, "Assessment of Brain Shift Related to Deep Brain Stimulation Surgery," *Stereotact Funct Neurosurgery,* vol. 86, pp. 44–53, 2008.

[5] C. H. Halpern, S. F. Danish, G. H. Baltuch, and J. L. Jaggi, "Brain Shift during Deep Brain Stimulation Surgery for Parkinson's Disease," *Stereotact Funct Neurosurg,* vol. 86, pp. 37–43, 2008.

[6] S. Pallavaram, P.-F. D'Haese, C. Kao, H. Yu, M. Remple, J. S. Neimat, P. E. Konrad, and B. M. Dawant, "A new method for creating electrophysiological maps for DBS surgery and their application to surgical guidance," in *LNCS (MICCAI), Part1.* vol. 5241: Springer-Verlag, 2008, p. 670:677.

[7] P.-F. D'Haese, E. Cetinkaya, P. E. Konrad, C. Kao, and B. M. Dawant, "Computer-Aided Placement of Deep Brain Stimulators: From Planning to Intraoperative Guidance," *IEEE Trans. on Medical Imaging,* vol. 24, pp. 1469-1478, 2005.

[8] P.-F. D'Haese, S. Pallavaram, H. Yu, J. Spooner, P. E. Konrad, and B. M. Dawant, "Deformable Physiological Atlas-Based Programming of Deep Brain Stimulators: A Feasibility Study," in *LNCS (WBIR).* vol. 4057 Utrecht, The Netherlands, 2006, p. 144:150.

[9] G. K. Rhode, A. Aldroubi, and B. M. Dawant, "The adaptive bases algorithm for intensity-based nonrigid image registration," *IEEE Trans. On Medical Imaging,* vol. 22:11, p. 1470:1479, 2003.

[10] C. R. Butson and C. C. McIntyre, "Current steering to control the volume of tissue activated during deep brain stimulation," *Brain Stimulation,* vol. 1:1, p. 7:15, 2008.